



HAL
open science

Nanosecond stochastic operation in perpendicular superparamagnetic tunnel junctions

Lucile Soumah, Louise Desplat, Nhat-Tan Phan, Ahmed Sidi El Valli, Advait Madhavan, Florian Disdier, Stéphane Auffret, Ricardo Sousa, Ursula Ebels, Philippe Talatchian

► **To cite this version:**

Lucile Soumah, Louise Desplat, Nhat-Tan Phan, Ahmed Sidi El Valli, Advait Madhavan, et al.. Nanosecond stochastic operation in perpendicular superparamagnetic tunnel junctions. 2024. hal-04666742

HAL Id: hal-04666742

<https://hal.science/hal-04666742v1>

Preprint submitted on 2 Aug 2024

HAL is a multi-disciplinary open access archive for the deposit and dissemination of scientific research documents, whether they are published or not. The documents may come from teaching and research institutions in France or abroad, or from public or private research centers.

L'archive ouverte pluridisciplinaire **HAL**, est destinée au dépôt et à la diffusion de documents scientifiques de niveau recherche, publiés ou non, émanant des établissements d'enseignement et de recherche français ou étrangers, des laboratoires publics ou privés.

Nanosecond stochastic operation in perpendicular superparamagnetic tunnel junctions

Lucile Soumah,^{1,*} Louise Desplat,^{2,1,*} Nhat-Tan Phan,¹ Ahmed Sidi El Valli,¹ Advait Madhavan,^{3,4} Florian Disdier,¹ Stéphane Auffret,¹ Ricardo Sousa,¹ Ursula Ebels,¹ and Philippe Talatchian^{1,†}

¹*Univ. Grenoble Alpes, CEA, CNRS, Grenoble INP, SPINTEC, 38000 Grenoble, France*

²*Nanomat/Q-mat/CESAM, Université de Liège, B-4000 Sart Tilman, Belgium*

³*Associate, Physical Measurement Laboratory, National Institute of Standards and Technology, Gaithersburg, Maryland 20899, USA*

⁴*Institute for Research in Electronics and Applied Physics, University of Maryland, College Park, Maryland 20742, USA*

(Dated: February 7, 2024)

We demonstrate the miniaturization of perpendicularly magnetized superparamagnetic tunnel junctions (SMTJs) down to 50 nm in diameter. We experimentally show stochastic reversals in those junctions, with tunable mean dwell times down to a few nanoseconds through applied magnetic field and voltage. The mean dwell times measured at negligible bias voltage agree with our simulations based on Langer’s theory. We shed light on an Arrhenius prefactor τ_0 of a few femtoseconds, implying that the rates of thermally-activated magnetic transitions exceed the GHz-to-THz limitation of macrospin models, whereby $\tau_0 \sim 1$ ns. We explain the small prefactor values by a Meyer-Neldel compensation phenomenon, where the prefactor exhibits a large entropic contribution with an exponential dependence on the activation energy. These findings pave the way towards the development of ultrafast, low-power unconventional computing schemes operating by leveraging thermal noise in perpendicular SMTJs, which are scalable below 20 nm.

In magnetism, mastering thermal activation is essential for understanding the complex interplay of temperature and magnetization dynamics that governs the behavior of spintronic nanostructures. On the one hand, enhancing thermal stability is crucial for preventing magnetization reversals in non-volatile memory with large data retention time [1–3]. On the other hand, reduced stability facilitates rapid magnetic state switchings, enabling numerous energy-efficient cognitive computing schemes [4, 5]. Controlling the susceptibility to thermal fluctuations in both regimes can be achieved by tailoring the magnetic energy landscape [6, 7]. In particular, according to the Arrhenius law, decreasing the energy barrier leads to an exponential reduction in retention time.

Magnetic tunnel junctions (MTJs) are a prime example of a device in which the study of thermally activated magnetization dynamics is important. MTJs consist of two ferromagnetic layers separated by an insulating oxide, and exhibit two metastable states, corresponding to the relative orientations of the magnetization in the two layers, namely, parallel (P), or antiparallel (AP). These states, readable through the tunneling magnetoresistance, have distinct resistance levels and are separated by an energy barrier. In particular, we refer to junctions in which thermal fluctuations induce random switchings between the two states at a scale ranging from tens of nanoseconds to seconds [6, 8, 9], as superparamagnetic tunnel junctions (SMTJs).

Despite the fact that SMTJs exhibit inherently stochastic resistance fluctuations between two configurations, the corresponding probability of being in a given

state can be controlled deterministically, using either an applied current that exerts spin-transfer torques on the magnetization [10–12], or by applying an external magnetic field. The tunable nature of SMTJs through external stimuli, coupled with their potential for very low energy consumption, has made them highly appealing for numerous low-energy cognitive applications. These include stochastic brain-inspired schemes [13], probabilistic computing [14, 15], as well as stochastic implementations of artificial neural networks [16].

A prospective strategy to further reduce energy consumption in these schemes is to shorten the mean dwell times between magnetization switching events, thereby reducing computing time without additional energy or area occupancy overheads. To this end, a straightforward approach is to reduce the energy barrier between magnetic states to a few kT_{RT} [17], in which k is Boltzmann’s constant, and T_{RT} is room temperature. So far, typical macrospin-based approaches have suggested that the mean waiting times between magnetization switching events—or mean dwell times—cannot be lower than an assumed characteristic attempt time, $\tau_0 \approx 0.1 - 1$ ns, even with negligible energy barriers, thus implying a notable speed limitation [6, 7].

Experimentally, the shortest dwell times of a few nanoseconds were reported in SMTJs with in-plane magnetization [8, 18, 19]. Their thermal stability is dominated by the shape anisotropy term and is therefore highly dependant on the shape of the junction. The latter is hard to control due to patterning-induced defects, when scaling down to nanometer dimensions.

To overcome the scaling challenge, perpendicular MTJs, i.e., with out-of-plane magnetization, are more promising candidates than their in-plane counterparts. This is due to their ability to be downscaled to sub-20 nm

* L. S. and L. D. contributed equally.

† philippe.talatchian@cea.fr

dimensions [20, 21], and the fact that they are commonly integrated into foundry industrial processes [22, 23], giving them a strategic integration advantage for future large-scale hardware deployments. While perpendicular structures have been extensively investigated as highly scalable building blocks for nonvolatile memory, there are only a few experimental reports of perpendicular SMTJs [24–27]. In these studies, the mean dwell times between thermally-induced magnetization switchings were reported at the hundreds of microseconds to millisecond scale, i.e., significantly slower than in their in-plane counterparts.

In this work, we report stochastic magnetization switching in perpendicular, 50 nm diameter SMTJs, with tunable mean dwell times down to the nanosecond timescale via the applied field or voltage, thus marking a significant advancement towards implementing both fast and scalable stochastic building blocks for low-energy cognitive computing. Our experimental demonstration is supported by micromagnetic computation of mean dwell times based on Langer’s theory [28, 29], beyond the typical macrospin model. The good agreement between experiment and simulation at low voltage challenges the traditional assumption of a 1 ns attempt time in nanodisks, and suggests that the Arrhenius prefactor in our junctions takes values in the tens of femtoseconds range. As we find that the computed dwell times obey the Meyer-Neldel compensation rule [30, 31], whereby the entropic contribution to the Arrhenius prefactor scales like an exponential of the activation energy [32–34], this hints at the fact that compensation may be occurring in our measured system, and constitutes the key mechanism behind the observed nanosecond dwell times.

The stack structure of the fabricated perpendicular SMTJs consists of Si substrate / SiO₂/Ta(15)/Pt(5)/[Co(0.5)/Pt(0.25)]₆/ Ru(0.9)/ [Co(0.5)/Pt(0.25)]₂/ Co(0.5) / W(0.25) / CoFeB(t_{fixed}) / MgO(1.25) / CoFeB(t_{free})/ W(2)/Pt(5). Numbers in parentheses represent thicknesses in nanometers, and subscripts on square brackets indicate the number of bilayer repeats. The two uniform, perpendicularly magnetized ferromagnetic layers of CoFeB, i.e., fixed and free, are separated by an insulating oxide layer (MgO).

To optimize the superparamagnetic behavior, we vary the CoFeB layer thicknesses through wedge deposition. We find the optimal thickness of the free layer to be $t_{\text{free}} = 1.6$ nm, yielding a minimal volume-averaged uniaxial anisotropy due to the interfacial perpendicular anisotropy [35], but sufficient to maintain the magnetization out of plane. For the fixed layer, the chosen thickness range of $t_{\text{fixed}} = 0.78 - 1.2$ nm allows us to reduce the applied field, while maintaining a large perpendicular magnetic anisotropy. Out-of-plane pinning of the magnetization in the fixed layer is ensured by exchange coupling with the synthetic antiferromagnetic structure of [Co(0.5)/Pt(0.25)]₆/ Ru(0.9)/ [Co(0.5)/Pt(0.25)]₂. Devices obtained after patterning are nearly circular, as illustrated in Fig. 1(a), with nominal diameters of 50 nm.

Their tunneling magnetoresistance (TMR) value is close to 70 % at room temperature, with a resistance-area product of $10 \Omega \mu\text{m}^2$.

We measure voltage fluctuations across the fabricated SMTJs using a high-bandwidth circuit designed to capture submicrosecond events, as described in the Supplemental Material (SM) [36]. The sampling rate of the high-resolution oscilloscope used for the measurement was set to 10 GHz, in order to match the RC circuit time constant of 0.2 ns [36].

Fig. 1(b) shows in blue an 80 ns long portion of a voltage-time trace recorded over 10 ms, under an applied perpendicular magnetic field of 40 mT, and 675 mV DC voltage across the circuit. The recorded signal distinctly exhibits a random telegraph noise (RTN) at the nanosecond scale. To ensure reliable statistics, we collected more than 10^6 stochastic transitions, allowing the identification of two distinct voltage levels, shown in the corresponding voltage histogram in Fig. 1(c). These are associated with low and high resistance states, respectively, consistent with P and AP magnetic configurations. The nanosecond dwell times are also confirmed in Fig. 1(d) by the autocorrelation function calculated over the entire recorded signal, which decays exponentially with a time constant of 5 ns. Additionally, we extract the individual dwell times from a digitized replica (red) of the analog voltage signal (blue) illustrated in Fig. 1(b). The resulting distributions are displayed in Figs. 1(e, f) as bin diagrams, and correspond to exponential distributions. The associated mean dwell times were found to be $\tau_{\text{AP}} = 8$ ns, and $\tau_{\text{P}} = 9$ ns, further supporting our claim of nanosecond stochastic operations in the studied SMTJ.

To demonstrate the tunability of the dwell times observed above, we apply a perpendicular magnetic field to modify the energy barrier $\Delta E_{\text{P(AP)}}$ separating the initial P(AP) state from the barrier top, as sketched in Fig. 2(a). For this purpose, we investigate a separate, nominally identical 50 nm diameter SMTJ. By varying the DC magnetic field from 0 to 150 mT, and the DC voltage across the SMTJ from approximately -400 to 360 mV, we uncover distinguishable RTN fluctuations, which we record systematically.

Following the procedure mentioned earlier, we extracted the mean dwell times for every recorded RTN signal. The results are summarized in Fig. 2(b). The obtained graph reveals a vast spectrum of switching timescales, from about 100 ns, to 0.1 ms. In particular, switchings were observed at the nanosecond timescale on both ends of the magnetic field range, i.e., below 10 mT, and above 150 mT, for voltage extremes of -400 and 360 mV. The latter were observed for voltages larger than roughly 200 mV, which highlights the crucial role of spin-transfer torques in enhancing the switching rates [6, 19]. Last, the longest mean dwell times of around 100 μs , are observed at fields near 50 mT, with less than 10 mV applied voltage, using a lower bandwidth setup [36] that captures dwell times exceeding one microsecond.

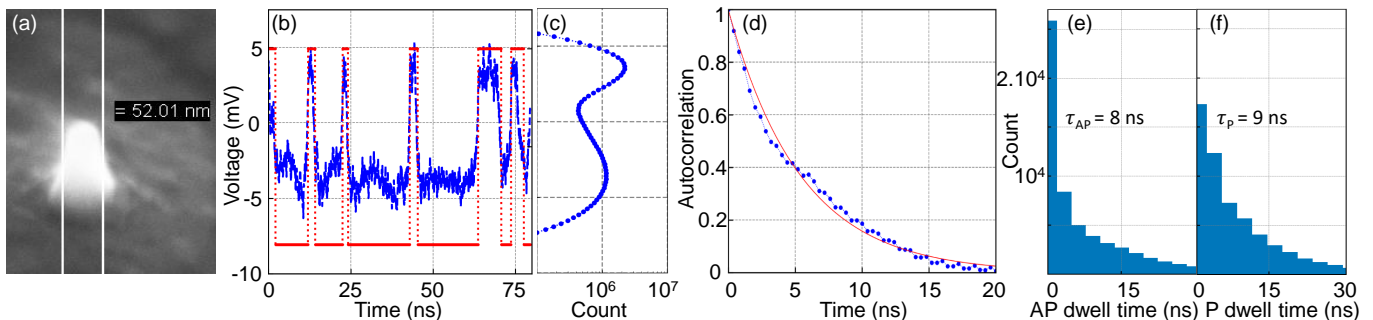


FIG. 1. (a) Scanning Electron Microscopy (SEM) image of a nominal 50 nm diameter perpendicular SMTJ pillar obtained after ion beam etching. (b) Random telegraph noise signal of a 50 nm diameter perpendicular SMTJ under an applied field of $\mu_0 H = 40$ mT, and DC voltage $V_{DC} = 675$ mV, for which the circuit is described in the SM [36]. An 80 ns portion of the recorded voltage-time trace exhibiting 10 transitions is shown in blue, together with its numerically digitized replica, shown in red. (c) Histogram of the overall voltage values measured over 10 ms and containing more than 10^6 transitions. (d) Autocorrelation function of the recorded voltage-time trace partially shown in (b) in blue, and with an exponential fit shown in red, with 5 ns autocorrelation time constant. (e, f) Histogram of (e) AP and (f) P dwell times collected from the digitized red signal in (b) of the overall voltage-time trace, corresponding to respectively 8 and 9 ns mean dwell times.

Fig. 2(b) additionally reveals an exponential variation of the collected mean dwell times, $\tau_{P(AP)}$, with the applied field H , at each value of the applied voltage. Since, as we show later in Fig. 3(b), $\Delta E_{P(AP)}$ is approximately linear in H , the observed exponential dependence of the mean dwell times on H is in line with the Arrhenius law,

$$\tau_{P(AP)} = \tau_0^{P(AP)} e^{\Delta E_{P(AP)}/kT_{RT}}, \quad (1)$$

in which kT_{RT} is the thermal energy at room temperature, and $\tau_0^{P(AP)}$ is a prefactor, commonly referred to as an attempt time.

Besides mean dwell time tunability, we show that the probability of occupying one of the two metastable states, such as the AP state, expressed as $P_{AP} = \tau_{AP}/(\tau_{AP} + \tau_P)$, can be tuned using the applied magnetic field, for every value of the operating voltage [36]. Fig. 2(c) shows that the evolution of P_{AP} with the field exhibits a distinct, nonlinear, sigmoid-like pattern. The tunable nature of the state probabilities constitutes a key feature for implementing adjustable stochastic, SMTJs-based binary neurons [13, 37].

To investigate the mechanism behind the observed dwell times, we perform micromagnetic simulations with a homemade code [30]. The parameters are that of a typical CoFeB free layer [38] with saturation magnetization $M_S = 1.03$ MA/m, spin stiffness $A = 10$ pJ/m, and Dzyaloshinskii-Moriya interaction (DMI) $D = 0.25$ mJ/m². We use a mesh size of $a = 1.4$ nm, for a total disk diameter of 46.2 nm and thickness of 1.4 nm. The perpendicular magnetic field, $\mu_0 H = \mu_0(H_{ext} - H_C)$, is varied from -10 to 10 mT, where H_{ext} is the applied field, and H_C is the experimental field at which $\tau_P = \tau_{AP}$. The effective anisotropy of the free layer can be roughly estimated in the range of 46 kJ/m³ [36] from the dimensions of the junction, and the values of the magnetic parameters reported in the literature for similar stacks [39]. In the simulations, we thus used three different values of

the net perpendicular anisotropy—including dipolar interactions: $K = 10.3, 15.5,$ and 43 kJ/m³.

Following the procedure described in [30, 40], we use the geodesic nudged elastic band method [41] to compute magnetization reversal pathways, and corresponding energy barriers, ΔE_P (see Fig. 2(a)). In agreement with previous studies, the reversal occurs through the nucleation and propagation of a domain wall through the disk [30, 38, 42, 43]. The saddle point configurations at $H = 0$ for the three considered anisotropy values are shown in Fig. 3(a), and the energy barriers as a function of applied field are given in Fig. 3(b) in units of the thermal energy, kT_{RT} , where $T_{RT} = 294$ K. Within the applied field range, the barrier approximately scales linearly with H [36].

The prefactor, τ_0^P in Eq. (1), is computed with Langer's theory [28, 29], as

$$\tau_0^P = \left(\frac{\lambda_+^P}{2\pi} \Omega_0^P \right)^{-1}, \quad (2)$$

in which Ω_0^P is the entropic contribution that contains the curvatures of the energy landscape at the initial and the transition state at the barrier top, and λ_+^P is the characteristic time associated with the unstable translation of the wall at the barrier top (see SM [36] for more details).

A formal limitation of this approach, in addition to those discussed elsewhere [30], is that the theory is formulated for equilibrium systems, in the sense that the density of states is assumed to be Boltzmann-distributed. Thus, it is not formally justified a priori, to compute dwell times at non-negligible applied currents, since the effect of the spin-transfer torques is expected to bring the system out of equilibrium. We therefore limit our comparison to experimental characterizations performed at the lowest voltage of $-9/-12$ mV (see red points in Fig. 2(b)).

The computed values of τ_0^P are presented in Fig. 3(c).

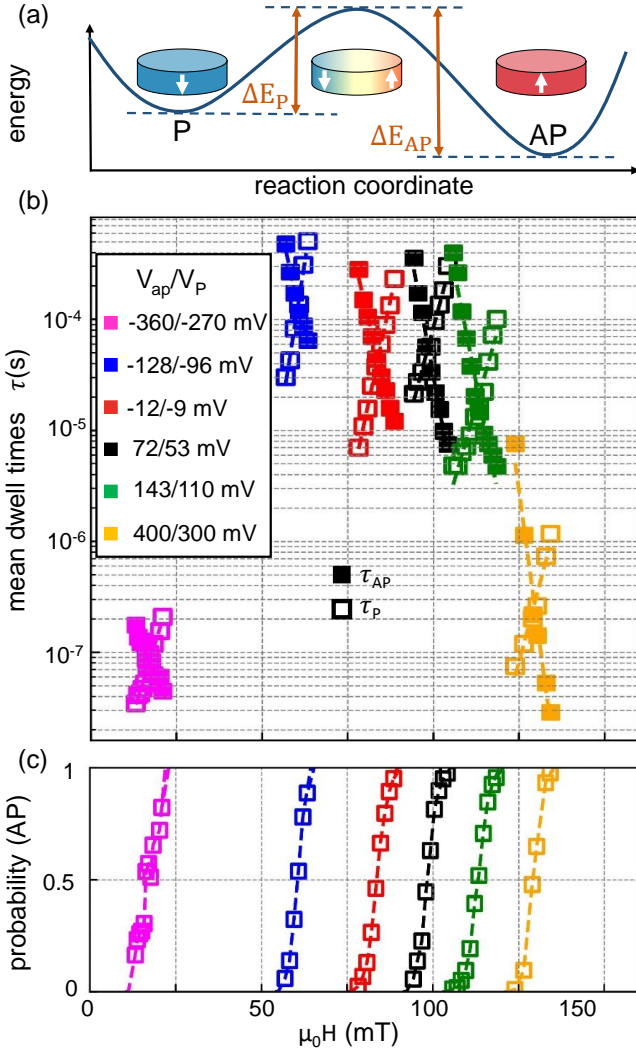


FIG. 2. (a) Sketch of the energy profile along the reaction coordinate for P and AP states, where the associated energy barriers are indicated as orange arrows. (b) Mean dwell times extracted for a 50 nm diameter device as a function of the perpendicular applied magnetic field, obtained for different voltages across the SMTJ, as described in the SM [36], and (c) corresponding probability of being in the AP state.

For the considered values of field and anisotropy, τ_0^P spans from a few femtoseconds to a few picoseconds, i.e., up to 6 orders of magnitude lower than the value of 1 ns typically considered in the literature [7, 38, 44–46]. These seemingly unphysical values stem from the larger number of states available to thermal fluctuations at the saddle point in the presence of a domain wall, compared to the metastable uniform state [30, 31]. This results in a large entropic contribution to the prefactor, which is contained in Ω_0^P . In that sense, the Arrhenius prefactor is not an attempt time. Moreover, for families of transitions obtained by varying the anisotropy, and the DMI, this system was shown to exhibit Meyer-Neldel compensation [30, 31], whereby $\tau_0 \propto e^{-\Delta E}$ [32–34]. In the inset

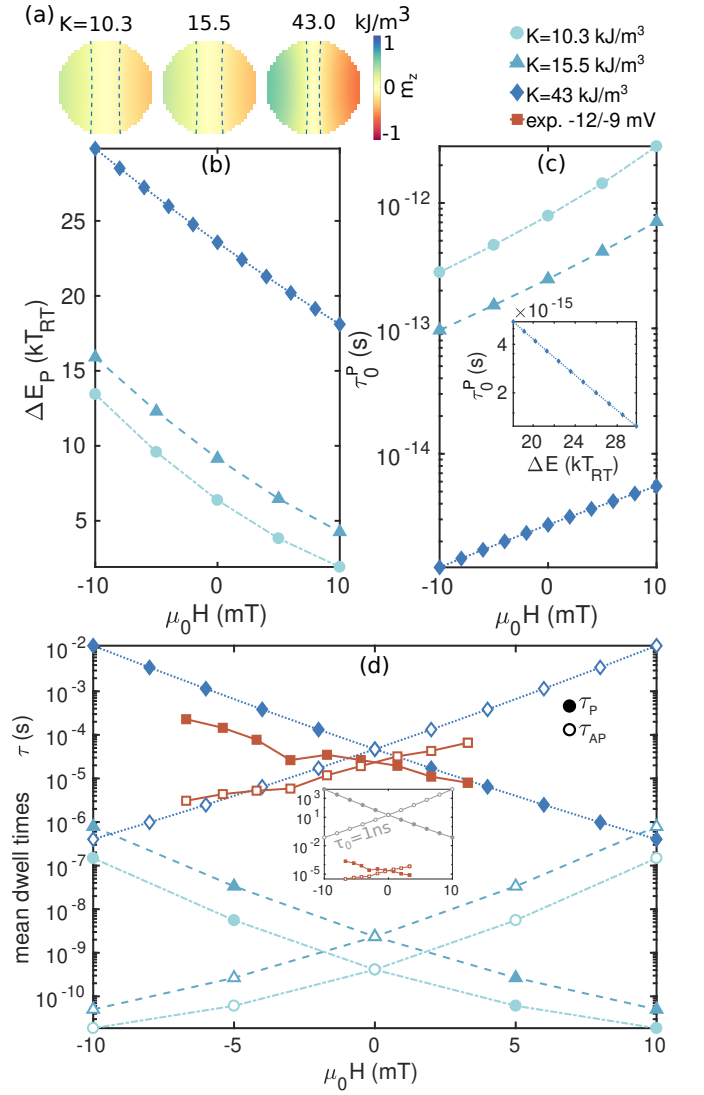


FIG. 3. Simulation results. (a) Saddle point configuration at three values of the anisotropy and zero applied field. The dashed isolines correspond to $m_z = \pm 0.1$ to indicate the position of the wall. (b, c, d) As a function of the applied magnetic field $\mu_0 H$ for three anisotropy values: (b) Energy barrier in units of the thermal energy at room temperature kT_{RT} , (c) Arrhenius prefactor, and (d) mean dwell times. The inset in (c) shows the prefactor as a function of the barrier in logarithmic scale for $K = 43$ kJ/m³, highlighting the compensation effect. The dwell times obtained experimentally are shown in (d) with red squares, and the inset shows a comparison with dwell times computed with the barriers in (b) and $\tau_0 = 1$ ns in gray.

of Fig. 3(c), τ_0^P is shown in logarithmic scale as a function of the energy barrier for $K = 43$ kJ/m³. The graph is approximately a straight line, implying that compensation also tends to occur when the magnetic field varies. For the lower values of K , however, compensation seems to progressively disappear with the lower barrier [32, 33].

The mean dwell times are computed with Eq. (1), and gathered in Fig. 3(d) for P and AP states, along with

the experimental values. Note that we only computed τ_P , and the values of τ_{AP} were obtained by observing, for a given value of H , $\tau_{AP}(-H) = \tau_P(H)$. On the one hand, for $K = 43 \text{ kJ/m}^3$, the computed dwell times agree well with the experimental values of tens of microseconds obtained at $-12/-9 \text{ mV}$, with $\Delta E_{P,AP} \sim 20 kT_{RT}$. In the inset of Fig. 3(d), we show that dwell times computed from the barriers in Fig. 3(b), and the assumption that $\tau_0^{P(AP)} = 1 \text{ ns}$ (in gray) fail to reproduce the measured dwell times (in red) by over 6 orders of magnitude. On the other hand, for lower values of K , the dwell times reach the (sub)nanosecond regimes, with energy barriers of the order of $10 kT_{RT}$. These findings demonstrate the possibility of achieving nanosecond scale mean dwell times in SMTJs, for sufficiently low values of K , even at low DC voltage.

As scalability is considered one of the appealing aspects of perpendicular MTJs, this raises the question of whether the timescales we measured will be preserved as the MTJs are scaled to smaller diameters. We have carried out simulations for a diameter of 20 nm and a larger anisotropy [36], indicating that the rapid switching behavior is maintained in this case. These simulations show that the reversal mode remains sufficiently distinct from coherent reversal that the effects reducing the prefactor in the measured system still play an important role, even at 20 nm.

In this work, we experimentally demonstrated stochastic magnetization switchings in perpendicularly magnetized, 50 nm diameter SMTJs. By fine-tuning the effective magnetic anisotropy, we showed that the fabricated SMTJs exhibit random telegraph noise, with dwell times as short as 8 ns—approximately four orders of magnitude shorter than those in traditional perpendicular SMTJs [24–26, 47]. The measured SMTJs also exhibit P(AP) state probabilities and mean dwell times that are both highly tunable with applied field and voltage. These characteristics constitute key ingredients towards the deployment of arrays of interacting, SMTJ-based, stochastic binary neurons at the nanoscale [37, 48].

While models based on the assumption that $\tau_0 \sim 1 \text{ ns}$ fail to predict the measured timescales, the conducted

simulations based on Langer’s theory successfully reproduce the trend of dwell times at negligibly small bias voltages. These simulations reveal an Arrhenius prefactor in the tens of femtoseconds range, in stark contrast to typical assumptions. This large reduction of the prefactor is the result of a Meyer-Neldel compensation phenomenon [30, 31], whereby the prefactor scales like an exponential of the energy barrier. This stems from the large entropic contribution yielded by the multiplicity of states available for the domain wall at the barrier top.

These findings showcase the necessity for more sophisticated theories encompassing multidimensional magnetic processes, beyond the macrospin approach. They imply that the timescale of thermally activated magnetic transitions expands beyond the GHz-to-THz regime, even for dimensions assumed to be compatible with the macrospin picture. Our work hereby paves the way towards the implementation of THz-operating stochastic units for cognitive computing, promising faster SMTJs with scalability down to tens of nanometers using perpendicular magnetic stacks.

Last, we note that properly understanding the equilibrium behavior of thermally-induced magnetization switchings in nanodisks is only the first step towards harnessing SMTJs for unconventional computing. Under applied currents, the dwell times of an array of junctions become coupled [48], and the whole system is driven out of equilibrium, thereby unlocking new emerging collective phenomena at the nanoscale.

ACKNOWLEDGEMENTS

We graciously thank Mark D. Stiles, Liliana Buda-Prejbeanu, Louis Hutin, and Olivier Fruchart for fruitful discussions and suggestions. NSF-ANR supported this work via grant StochNet Project ANR-21-CE94-0002-01. This work was partially supported by NSF grant number CCF-CISE-ANR-FET-2121957, the Carnot project PRIME SPORT ANR P-22-03813, and the French RENATECH network. L. D. acknowledges funding from the University of Liège under Special Funds for Research, IPD-STEMA Programme.

-
- [1] S. Bhatti, R. Sbiaa, A. Hirohata, H. Ohno, S. Fukami, and S. Piramanayagam, Spintronics based random access memory: a review, *Materials Today* **20**, 530 (2017).
 - [2] B. Dieny, I. L. Prejbeanu, K. Garello, P. Gambardella, P. Freitas, R. Lehdorff, W. Raberg, U. Ebels, S. O. Demokritov, J. Akerman, *et al.*, Opportunities and challenges for spintronics in the microelectronics industry, *Nature Electronics* **3**, 446 (2020).
 - [3] A. D. Kent and D. C. Worledge, A new spin on magnetic memories, *Nature nanotechnology* **10**, 187 (2015).
 - [4] J. Grollier, D. Querlioz, K. Camsari, K. Everschor-Sitte, S. Fukami, and M. D. Stiles, Neuromorphic spintronics, *Nature electronics* **3**, 360 (2020).
 - [5] B. Cai, Y. He, Y. Xin, Z. Yuan, X. Zhang, Z. Zhu, and G. Liang, Unconventional computing based on magnetic tunnel junction, *Applied Physics A* **129** (2023).
 - [6] W. Rippard, R. Heindl, M. Pufall, S. Russek, and A. Kos, Thermal relaxation rates of magnetic nanoparticles in the presence of magnetic fields and spin-transfer effects, *Phys. Rev. B* **84**, 064439 (2011).
 - [7] S. Kanai, K. Hayakawa, H. Ohno, and S. Fukami, Theory of relaxation time of stochastic nanomagnets, *Phys. Rev. B* **103**, 094423 (2021).

- [8] K. Hayakawa, S. Kanai, T. Funatsu, J. Igarashi, B. Jinnai, W. Borders, H. Ohno, and S. Fukami, Nanosecond random telegraph noise in in-plane magnetic tunnel junctions, *Phys. Rev. Lett.* **126**, 117202 (2021).
- [9] D. Vodenicarevic, N. Locatelli, A. Mizrahi, J. S. Friedman, A. F. Vincent, M. Romera, A. Fukushima, K. Yakushiji, H. Kubota, S. Yuasa, S. Tiwari, J. Grollier, and D. Querlioz, Low-energy truly random number generation with superparamagnetic tunnel junctions for unconventional computing, *Phys. Rev. Appl.* **8**, 054045 (2017).
- [10] L. Berger, Emission of spin waves by a magnetic multilayer traversed by a current, *Phys. Rev. B* **54**, 9353 (1996).
- [11] J. C. Slonczewski, Current-driven excitation of magnetic multilayers, *J. Magn. Magn. Mater.* **159**, L1 (1996).
- [12] D. C. Ralph and M. D. Stiles, Spin transfer torques, *J. Magn. Magn. Mater.* **320**, 1190 (2008).
- [13] A. Mizrahi, T. Hirtzlin, A. Fukushima, H. Kubota, S. Yuasa, J. Grollier, and D. Querlioz, Neural-like computing with populations of superparamagnetic basis functions, *Nature communications* **9**, 1533 (2018).
- [14] W. A. Borders, A. Z. Pervaiz, S. Fukami, K. Y. Camsari, H. Ohno, and S. Datta, Integer factorization using stochastic magnetic tunnel junctions, *Nature* **573**, 390 (2019).
- [15] N. A. Aadit, A. Grimaldi, M. Carpentieri, L. Theogarajan, J. M. Martinis, G. Finocchio, and K. Y. Camsari, Massively parallel probabilistic computing with sparse ising machines, *Nature Electronics* **5**, 460 (2022).
- [16] M. W. Daniels, A. Madhavan, P. Talatchian, A. Mizrahi, and M. D. Stiles, Energy-efficient stochastic computing with superparamagnetic tunnel junctions, *Physical review applied* **13** **3** (2019).
- [17] R. Faria, K. Y. Camsari, and S. Datta, Low-barrier nanomagnets as p -bits for spin logic, *IEEE Magnetics Letters* **8**, 1 (2017).
- [18] C. Safranski, J. Kaiser, P. Trouilloud, P. Hashemi, G. Hu, and J. Z. Sun, Demonstration of nanosecond operation in stochastic magnetic tunnel junctions, arXiv preprint arXiv:2010.14393 (2020).
- [19] L. Schnitzspan, M. Kläui, and G. Jakob, Nanosecond true-random-number generation with superparamagnetic tunnel junctions: Identification of joule heating and spin-transfer-torque effects, *Phys. Rev. Appl.* **20**, 024002 (2023).
- [20] N. Caçoilo, S. Lequeux, N. Strelkov, B. Diény, R. C. Sousa, N. A. Sobolev, O. Fruchart, I. L. Prejbeanu, and L. D. Buda-Prejbeanu, Spin-Torque-Triggered Magnetization Reversal in Magnetic Tunnel Junctions with Perpendicular Shape Anisotropy, *Physical Review Applied* **16**, 024020 (2021), 5 pages with a total of 7 figures.
- [21] B. Jinnai, K. Watanabe, S. Fukami, and H. Ohno, Scaling magnetic tunnel junction down to single-digit nanometers—challenges and prospects, *Appl. Phys. Lett.* **116**, 160501 (2020).
- [22] S. Jung, H. Lee, S. Myung, H. Kim, S. K. Yoon, S.-W. Kwon, Y. Ju, M. Kim, W. Yi, S. Han, *et al.*, A crossbar array of magnetoresistive memory devices for in-memory computing, *Nature* **601**, 211 (2022).
- [23] S. Sakhare, M. Perumkunnil, T. H. Bao, S. Rao, W. Kim, D. Crotti, F. Yasin, S. Couet, J. Swerts, S. Kundu, *et al.*, Enablement of stt-mram as last level cache for the high performance computing domain at the 5nm node, in *2018 IEEE International Electron Devices Meeting (IEDM)* (IEEE, 2018) pp. 18–3.
- [24] B. Parks, M. Bapna, J. Igbokwe, H. Almasi, W. Wang, and S. Majetich, Superparamagnetic perpendicular magnetic tunnel junctions for true random number generators, *AIP Advances* **8**, 055903 (2017).
- [25] T. Funatsu, S. Kanai, J. Ieda, S. Fukami, and H. Ohno, Local bifurcation with spin-transfer torque in superparamagnetic tunnel junctions, *Nature communications* **13**, 4079 (2022).
- [26] K. Kobayashi, W. A. Borders, S. Kanai, K. Hayakawa, H. Ohno, and S. Fukami, Sigmoidal curves of stochastic magnetic tunnel junctions with perpendicular easy axis, *Applied Physics Letters* **119**, 132406 (2021), https://pubs.aip.org/aip/apl/article-pdf/doi/10.1063/5.0065919/14554384/132406_1_online.pdf.
- [27] M. Bapna and S. A. Majetich, Current control of time-averaged magnetization in superparamagnetic tunnel junctions, *Applied Physics Letters* **111**, 243107 (2017), https://pubs.aip.org/aip/apl/article-pdf/doi/10.1063/1.5012091/13155126/243107_1_online.pdf.
- [28] J. S. Langer, Statistical theory of the decay of metastable states, *Annals of Physics* **54**, 258 (1969).
- [29] W. T. Coffey and Y. P. Kalmykov, Thermal fluctuations of magnetic nanoparticles: Fifty years after brown, *Journal of Applied Physics* **112**, 121301 (2012).
- [30] L. Desplat and J.-V. Kim, Entropy-reduced retention times in magnetic memory elements: A case of the meyer-neldel compensation rule, *Phys. Rev. Lett.* **125**, 107201 (2020).
- [31] L. Desplat and J.-V. Kim, Quantifying the thermal stability in perpendicularly magnetized ferromagnetic nanodisks with forward flux sampling, *Phys. Rev. Appl.* **14**, 064064 (2020).
- [32] E. Peacock-Lopez and H. Suhl, Compensation effect in thermally activated processes, *Physical Review B* **26**, 3774 (1982).
- [33] A. Yelon and B. Movaghar, Microscopic explanation of the compensation (meyer-neldel) rule, *Physical Review Letters* **65**, 618 (1990).
- [34] A. Yelon, B. Movaghar, and H. M. Branz, Origin and consequences of the compensation (meyer-neldel) law, *Physical Review B* **46**, 12244 (1992).
- [35] B. Dieny and M. Chshiev, Perpendicular magnetic anisotropy at transition metal/oxide interfaces and applications, *Reviews of Modern Physics* **89**, 025008 (2017).
- [36] See supplemental material at url will be inserted by publisher, .
- [37] N.-T. Phan, L. Soumah, A. Sidi El Valli, L. Hutin, L. Anghel, U. Ebels, and P. Talatchian, Electrical coupling of perpendicular superparamagnetic tunnel junctions for probabilistic computing, in *Proceedings of the 17th ACM International Symposium on Nanoscale Architectures*, NANOARCH '22 (Association for Computing Machinery, New York, NY, USA, 2023).
- [38] J. Sampaio, A. Khvalkovskiy, M. Kuteifan, M. Cubukcu, D. Apalkov, V. Lomakin, V. Cros, and N. Reyren, Disruptive effect of dzyaloshinskii-moriya interaction on the magnetic memory cell performance, *Applied Physics Letters* **108**, 112403 (2016).
- [39] J. Chatterjee, *Engineering of magnetic tunnel junction stacks for improved STT-MRAM performance and development of novel and cost-effective nano-patterning techniques*, *Theses*, Université Grenoble Alpes (2018).

- [40] L. Desplat, D. Suess, J.-V. Kim, and R. L. Stamps, Thermal stability of metastable magnetic skyrmions: Entropic narrowing and significance of internal eigenmodes, *Physical Review B* **98**, 134407 (2018).
- [41] P. F. Bessarab, V. M. Uzdin, and H. Jonsson, Method for finding mechanism and activation energy of magnetic transitions, applied to skyrmions and antivortex annihilation, *Computer Physics Communications* **196**, 335 (2015).
- [42] A. Khvalkovskiy, D. Apalkov, S. Watts, R. Chepulskii, R. Beach, A. Ong, X. Tang, A. Driskill-Smith, W. Butler, P. Visscher, *et al.*, Basic principles of stt-mram cell operation in memory arrays, *Journal of Physics D: Applied Physics* **46**, 074001 (2013).
- [43] P.-H. Jang, K. Song, S.-J. Lee, S.-W. Lee, and K.-J. Lee, Detrimental effect of interfacial dzyaloshinskii-moriya interaction on perpendicular spin-transfer-torque magnetic random access memory, *Applied Physics Letters* **107**, 202401 (2015).
- [44] D. Weller and A. Moser, Thermal effect limits in ultrahigh-density magnetic recording, *IEEE Transactions on Magnetics* **35**, 4423 (1999).
- [45] E. Chen, D. Apalkov, Z. Diao, A. Driskill-Smith, D. Druist, D. Lottis, V. Nikitin, X. Tang, S. Watts, S. Wang, *et al.*, Advances and future prospects of spin-transfer torque random access memory, *IEEE Transactions on Magnetics* **46**, 1873 (2010).
- [46] M. Lederman, S. Schultz, and M. Ozaki, Measurement of the dynamics of the magnetization reversal in individual single-domain ferromagnetic particles, *Physical Review Letters* **73**, 1986 (1994).
- [47] M. Bapna and S. A. Majetich, Current control of time-averaged magnetization in superparamagnetic tunnel junctions, *Appl. Phys. Lett.* **111**, 243107 (2017).
- [48] P. Talatchian, M. W. Daniels, A. Madhavan, M. R. Puffall, E. Jué, W. H. Rippard, J. J. McClelland, and M. D. Stiles, Mutual control of stochastic switching for two electrically coupled superparamagnetic tunnel junctions, *Physical Review B* **104**, 054427 (2021).